Available online at www.sciencedirect.com
ScienceDirect
Surface Science 601 (2007) 2291–2296
SURFACE SCIENCE
www.elsevier.com/locate/susc

The molecular orientation of DNA bases on H-passivated Si(1 1 1) surfaces investigated by means of near edge X-ray absorption fine structure spectroscopy

Stefan Seifert [a,*], Gianina N. Gavrila [a], Dietrich R.T. Zahn [a], Walter Braun [b]

[a] *Institut für Physik, Technische Universität Chemnitz, D-09107 Chemnitz, Germany*
[b] *BESSY GmbH, Albert-Einstein-Str. 15, D-12489 Berlin, Germany*

Received 11 October 2006; accepted for publication 10 January 2007
Available online 24 January 2007

Abstract

Layers of the DNA bases adenine, cytosine, and guanine were deposited onto hydrogen passivated Si(1 1 1) surfaces. The average tilt angles of these molecules with respect to the substrate surface were determined by the angular dependence of the Near Edge X-ray Absorption Fine Structure (NEXAFS) of the carbon K-edge. The interpretation of the NEXAFS spectra was assisted by a semi-empirical approach to the calculation of the π^*-transition region which employs density functional theory calculations and core level photoemission data.

Keywords: DNA base; Adenine; Cytosine; Guanine; Molecular orientation; Near edge X-ray absorption fine structure spectroscopy; NEXAFS; Core level; Photoemission spectroscopy

1. Introduction

In recent years DNA bases as well as DNA molecules have been discussed as promising materials in electronic applications that connect conventional inorganic electronics with biological relevant materials. The variety of possible applications reaches from (bio-)organic field effect transistors [7] to molecular nano-wires [11]. The performance of such devices largely depends on the conductivity of the materials and the charge injection across interfaces. The strong anisotropy of the charge transport properties within molecular crystals leads to a strong dependence of the overall device efficiency on the molecular orientation. This makes the knowledge of the orientation of the DNA bases with respect to substrates and contacts crucial for device design. A well established tool to determine the orientation of π-conjugated molecules on surfaces is the angular dependence of NEXAFS spectra. Crain et al. [2] made an attempt to determine the orientation of DNA segments on Au, Si and SiO_2 surfaces but a relatively low degree of ordering of the DNA molecules prevented the precise determination of tilt angles. Therefore, a systematic NEXAFS study of the carbon K-edge of layers of the DNA bases adenine, cytosine, and guanine on H-passivated Si(1 1 1) surfaces was performed.

2. Experimental

2.1. Sample preparation

The Si substrates were cut from n-type, phosphor doped silicon(1 1 1) wafers (resistivity 7.5 Ω cm) supplied by SilChem GmbH. The DNA bases adenine, cytosine and guanine were used as purchased from Acros Organics (purity 99% in the case of cytosine and guanine; 99.5% for

* Corresponding author.
E-mail address: stefan.seifert@physik.tu-chemnitz.de (S. Seifert).

0039-6028/$ - see front matter © 2007 Elsevier B.V. All rights reserved.
doi:10.1016/j.susc.2007.01.022

adenine). The samples were first annealed by resistive heating at 450 °C under ultra-high vacuum (UHV) conditions (base pressure $\leqslant 3 \times 10^{-10}$ mbar). The annealing temperature was further increased by direct current (DC) heating up to 750–800 °C. The natural oxide was removed by several DC flushes of 20 s duration up to 1100–1300 °C. Then the substrates were cooled down slowly to preserve the (7×7) reconstruction [10,18]. The surface was passivated in situ by exposure to (2.0 ± 0.5) Langmuir of hydrogen. This dose was chosen carefully to saturate the dangling bonds of the Si(1 1 1)(7×7) while preserving the reconstruction. The H:Si(1 1 1)(7×7) surfaces prepared by this method showed a considerably lower surface roughness than achieved by a wet-chemical cleaning and passivation treatment of Si(1 1 1). The DNA base layers were deposited by organic molecular beam deposition (OMBD). For each DNA base several layers with varying thicknesses starting from 1 nm up to 10 nm were prepared and analyzed. The nominal layer thickness was monitored using a quartz microbalance. The quartz shift to thickness ratio was calibrated separately for each material by means of variable angle spectroscopic ellipsometry. In this report, however, only the data for the 10 nm thick layers are presented as no significant differences could be observed in the spectra of the thinner films.

2.2. Measurements

All measurements were performed at the Russian German Beam line of the synchrotron radiation source BESSY (Berlin). The core level photoemission spectra (CL-PES) were recorded using the MUSTANG experimental station equipped with a Phoibos 150 electron energy analyzer (SPECS GmbH). All the carbon core levels were recorded in surface sensitive conditions using an excitation energy of 335 eV. The overall resolution of the setup at this energy can be estimated to be better than 0.12 eV. Decomposition of the molecules upon irradiation could be excluded since no changes in core level emission spectra as a function of time were observed. The NEXAFS spectra were recorded in the selected electron yield mode in the region of the secondary electron background (i.e. at a kinetic energy of 10 eV) using the same experimental station. The angle of incidence, Θ, between the incident light and the sample surface was varied between of 22° and 115°. The measured data were normalized to the photon flux by dividing each spectrum by the electron yield spectrum of the clean H:Si(1 1 1)(7×7) sample and the synchrotron ring current. A constant background was subtracted before finally normalizing the spectra to the absorption step edge at 320 eV.

For a better interpretation of the spectra, the ground state eigenenergies were calculated for single molecules by a density functional theory (DFT) approach using the commercial software package Gaussian'03 [3]. The calculations were performed employing B3LYP [1,15] three parameter mixed hybrid functionals with 6-311G + (d, p) polarized, diffuse basis sets.

3. Results and discussion

3.1. The carbon 1s CL-PES

In Fig. 1 the measured C 1s CL-PES of the adenine, guanine, and cytosine layers are displayed. In order to analyze the spectra Voigt-functions were fitted to the experimental data using a Marquardt nonlinear least square optimization algorithm. In a first step the peak parameters were approximated using as few free parameters as possible. For the C 1s core levels the full widths at half maximum (FWHM) of the Lorentzian contribution (representing the lifetime of the final state) were fixed to 80 meV [13]. The FWHM of the Gaussian contributions were coupled to be equal for all components. Additionally the area ratio of the different components in the spectra was fixed to represent the stoichiometry of the molecules. Here one has to take into account that a considerable contribution of the area goes into the clearly visible shake-up satellites [13].

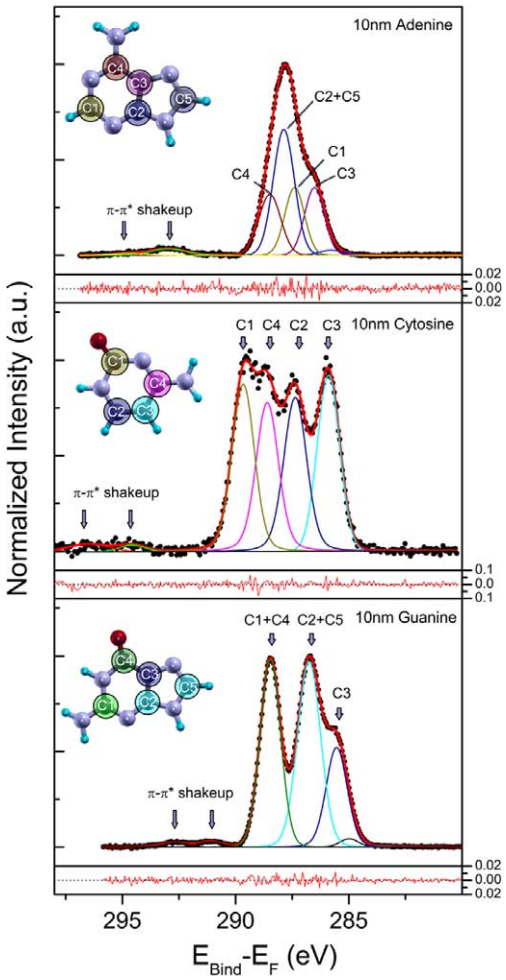

Fig. 1. C 1s CL-PES of the DNA bases adenine, cytosine, and guanine. The experimental data were deconvoluted into the contribution of different carbon atoms by the fitting procedure described in the text. The residuals are shown below each spectrum. The assignment of the peaks to individual C-atoms is based on theoretical calculations of the ground state eigenenergies for single molecules as described in the text.

For example, the peak area ratio in the adenine C 1s CL-PES (see top Fig. 1) was fixed to

$$\mathrm{area(C1)} : \mathrm{area(C2)} : \mathrm{area(C3 + shakeup1)} : \mathrm{area(C4 + shakeup2)} = 1 : 1 : 2 : 1$$

The resulting peak positions were found to be perfectly reproducible within the experimental resolution. In a second step, the restrictions to the FWHM (Lorentzian and Gaussian) of the separate peaks were released resulting, however, in only minimal changes. The peak positions and relative areas obtained by this method are summarized in Table 1 for the main features in the spectra. These peaks were assigned to individual carbon atoms following the theoretically calculated ground state eigenenergies.

The small components at low binding energy visible in the spectra obtained for adenine and guanine layers on H:Si(1 1 1)(7 × 7) are most likely due to some residual carbon contamination on the substrate surfaces. The nominal layer thickness of 10 nm exceeds the information depth of the measurement of approx. 0.6 nm by more than one order of magnitude. The fact that surface contamination is still visible in the CL-PES spectra of the 10 nm thick adenine and guanine layers suggests a pronounced island growth for these layers.

3.2. Analysis of the NEXAFS spectra

Fig. 2 shows the NEXAFS spectra of the carbon K-edge measured on layers of the DNA bases adenine, cytosine and guanine as a function of the angle of incidence, Θ. The sharp peaks below the absorption step edge are attributed to C 1s → π* transitions. In order to determine the molecular orientation of the DNA bases one has to know the orientation of the corresponding transition dipole which is related to the symmetry of the final state because the initial state (1s) is spherically symmetric. One simple picture that is often used to classify molecules into general groups according to the relative orientation of their unoccupied orbitals was introduced by Stöhr and Outka [17]. Because of the localized nature of the 1s initial state, the dominating elements of the one-electron dipole transition matrix should be predominantly determined by the contribution of the atomic orbitals (AO) of the excited atom to the molecular orbitals (MOs) [16]. This allows the decomposition of complex molecules into diatomic units as illustrated in Fig. 3.

Table 1
Peak positions and relative areas of the most prominent features in the C 1s CL-PES

DNA-base	Component	Peak position (eV)	Rel. peak area
Adenine	C3	286.5 ± 0.12	0.20
	C1	287.4 ± 0.12	0.20
	C2 + C5	287.9 ± 0.12	0.35
	C4	288.5 ± 0.12	0.19
Cytosine	C3	285.9 ± 0.12	0.25
	C2	287.3 ± 0.12	0.24
	C4	288.6 ± 0.12	0.23
	C1	289.7 ± 0.12	0.25
Guanine	C3	285.5 ± 0.12	0.20
	C2 + C5	286.7 ± 0.12	0.40
	C1 + C4	288.4 ± 0.12	0.36

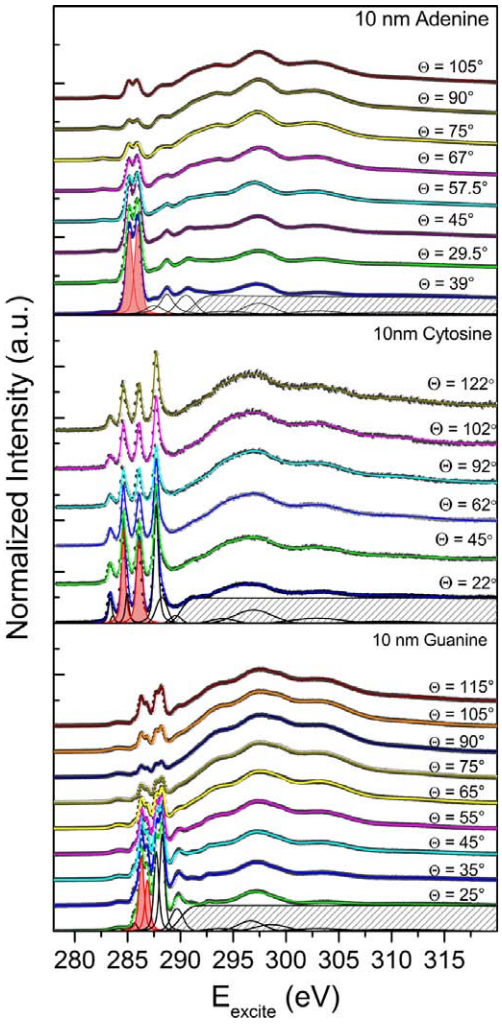

Fig. 2. The carbon K-edge NEXAFS spectra of 10 nm adenine (top), cytosine (middle), and guanine (bottom) on H:Si(1 1 1)(7 × 7) as a function of the angle of incidence, Θ. Circles represent the measured data and lines the fitted curves. The individual components of the fits are exemplary included in the bottom spectra.

DFT calculations display the MOs as the result of a linear combination of AOs. Therefore, such calculations allow access to the contribution of individual atoms to the MOs and provide an ideal tool to test the assumption of the strongly localized nature of the NEXAFS transitions. Unfortunately the density of unoccupied states of the calculated ground state cannot directly be compared to the NEXAFS spectra for two reasons. First the binding energy of the 1s initial state is not equal for the different carbon atoms of the DNA bases, as can be easily seen in Fig. 1. Secondly the excitation leaves one electron less in the 1s shell of the excited atom to screen the core potential. This so called core hole has a profound impact on the remaining

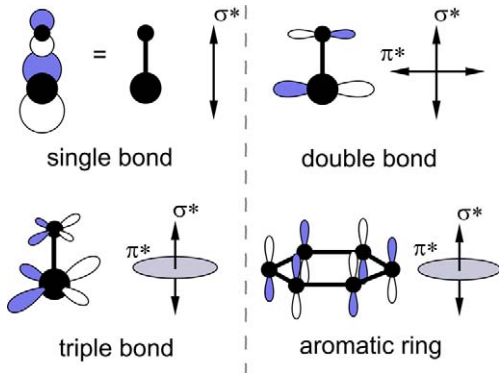

Fig. 3. Schematic illustration of the spatial orientation of the anti-bonding π^* and σ^* orbitals for three classes of diatomic molecules. The combination of three single and three double bond units leads to the configuration of the aromatic ring [17].

molecular orbitals in molecules as small as the DNA bases. This effect can be strongly site dependent giving rise to different final states of the excitation of different atoms [9,12].

In order to take these effects into account a semi-empirical approach was used to simulate the $1s \rightarrow \pi^*$-transition region of the NEXAFS spectra. It is based on the $Z+1$ (also called equivalent core) approximation, which was applied by Nyberg et al. successfully to calculate the X-ray absorption spectra of fullerenes [8]. There the influence of the vacancy in the 1s shell of the excited atom on the molecular orbitals is approximated by increasing the positive charge of the nucleus by one unit instead of removing the 1s electron. Therefore, an excited atom with the atomic number Z ($Z = 6$ for carbon) is replaced by an atom with the atomic number $Z+1$ (i.e. nitrogen). The following DFT calculation is performed for a positively charged molecule in order to keep the number of electrons constant. Naturally the $Z+1$ approximation cannot produce reliable results for the 1s initial state energy which is therefore replaced by the measured C 1s core level ionization potential (CL-IP) for the calculation of the transition energies. Assuming vertical transitions from the 1s initial state into the unoccupied MOs the transition energies are then given by the difference between CL-IP and the calculated unoccupied molecular orbitals. Finally, these molecular orbitals were decomposed into the contributing atomic orbitals using the AOMix program [5,4]. Following the above argumentation, that the one-electron dipole transition matrix is determined by the AOs, the intensity is given by the contribution of the $2p_z$ (anti-bonding) AO to the population of the unoccupied MOs. Each excitation site was treated separately by this procedure. The contributions of all the carbon atoms within the molecule are averaged and broadened using Voigt functions having a FWHM of 0.3 eV. A comparison between the calculated π^*-transitions and the NEXAFS spectra below the vacuum step edge is shown in Fig. 4. The calculated spectra were shifted by $\Delta E_A = 2.86$ eV, $\Delta E_C = 4.36$ eV, and $\Delta E_G = 2.87$ eV towards higher excitation energies in order to match the peaks at lower excitation energies. Such relatively large

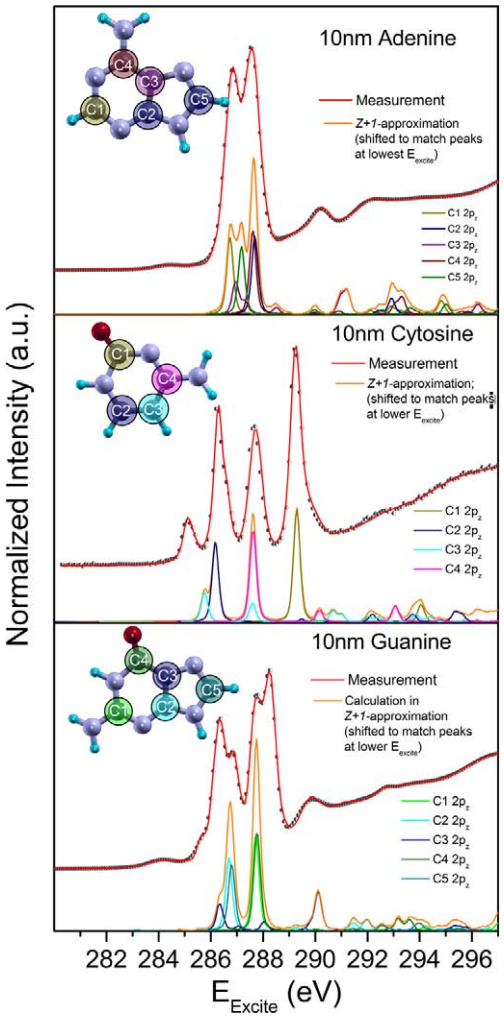

Fig. 4. Comparison between the measured NEXAFS spectra ($\Theta = 45°$) and the calculations in the $Z+1$ approximation. The calculated spectra were shifted by $\Delta E_A = 2.86$ eV, $\Delta E_C = 4.36$ eV, and $\Delta E_G = 2.87$ eV towards higher excitation energies.

shifts are caused by the fact that the extra positive charge on the molecule is introducing an additional shift of all molecular orbitals towards higher binding energies. At this point it must be stressed again that these calculations only consider the density of states and the Coulomb interaction between a core hole and the molecular orbitals. Other effects such as the generation of bound electron hole pairs (excitons) are neglected and therefore, especially in the case of guanine, there are still some dissimilarities between the calculated spectra and the measured data. Nevertheless, the calculations resemble the shape of the π^*-transition region of the measured NEXAFS spectra very well and we can say that the assumption of the strongly localized nature of the π^*-transitions is justified.

3.3. Molecular orientation

For the quantitative analysis of the angular dependence of the NEXAFS spectra three different types of functions

were used to fit the experimental data. For the peaks below the vacuum level Voigt functions were chosen. An error function was used to model the step which marks the transition to quasi-continuous final states [16]. The broad features above the step edge were represented by Gaussian functions. The individual components of the fits of the measurements at grazing incidence are displayed in Fig. 2. The areas of those π*-transition peaks, that are marked with the solid shading in Fig. 2, were then used to determine the molecular orientation of the DNA bases.

The dependence of the resonance intensity on the angle of incidence, under the condition of threefold (or higher) substrate symmetry is given by [17]

$$I = C[P(\cos^2\Theta\cos^2\alpha + 1/2\sin^2\Theta\sin^2\alpha) + (1-P)/2\sin^2\alpha], \quad (1)$$

where P is the polarization factor ($P = 0.98$) and C is a normalization factor. Θ is the angle of incidence and α the angle between the transition dipole moment and the surface normal. As described above and illustrated in Fig. 5a, the transition dipole moment is in the case of the π*-resonances, oriented parallel to the $2p_z$ AOs, i.e. perpendicular to the molecular planes. It is easy to see, that in this geometry the molecular tilt angle is equal to α.

The angle Θ and the polarization factor for the exciting beam are known quantities, which only leaves the molecular orientation and the normalization constant C unknown. These parameters can be determined by curve fitting equation (1) to the relative intensities of the π*-resonances in the NEXAFS spectra. The fitted curves are presented in Fig. 5b. The average molecular tilt angles of the DNA base molecules with respect to the substrate surface are determined to be

$$\alpha_A = (24 \pm 3^\circ); \quad \alpha_C = (39.6 \pm 1.5^\circ); \quad \alpha_G = (25.8 \pm 1.3^\circ).$$

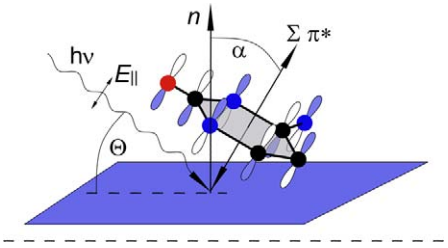

Fig. 5a. Scheme of the geometry used to determine the molecular orientation of the DNA bases on H:Si(1 1 1)(7 × 7).

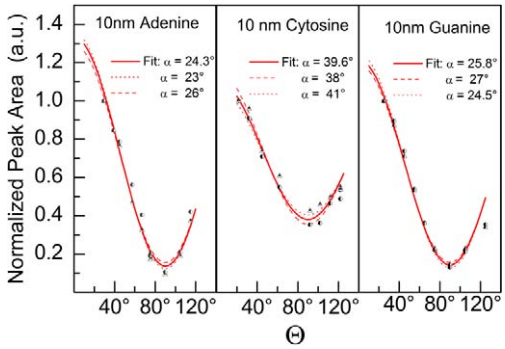

Fig. 5b. Symbols indicate the normalized areas (see text) of selected π-transition peaks (solid shading in Fig. 2) in the NEXAFS spectra of adenine (left), cytosine (middle) and guanine (right) as a function of the angle of incidence. By variation of α and C to optimize the match between measurement and Eq. (1) the average molecular orientation of each DNA base is obtained.

4. Summary

The carbon 1s core level spectra of the DNA bases adenine, cytosine; and guanine were measured and deconvoluted by curve fitting according to the stoichiometry of the molecules. The C 1s core level binding energies were then used in the semi-empirical $Z + 1$ approximation to simulate the $1s \rightarrow \pi^*$-transitions in the carbon K-edge NEXAFS spectra. Due to the drastic simplifications employed, this method has to be used very carefully. The good agreement between the simulated spectra and the measured data for the DNA bases, however, shows that it can be a useful tool for the evaluation of NEXAFS data while avoiding the use of non-standard software.

The angular dependence of the π*-transition intensities of the NEXAFS spectra was used to determine the average molecular tilt angle of the DNA bases with respect to the H:Si(1 1 1)(7 × 7) surface. The pyrimidine bases adenine and guanine assume similar orientations and lay almost flat on the substrate surface ($\alpha_A = [24 \pm 3°]$ and $\alpha_G = [25.8 \pm 1.3°]$). Cytosine on the other hand is tilted more upright ($\alpha_C = [39.6 \pm 1.5°]$). These angles are in excellent agreement with results obtained from Fourier transform infrared spectroscopy and spectroscopic ellipsometry [14,19,6]. To clarify the origin of the difference between the purine bases and the pyrimidine cytosine more data is needed (especially from other purines such as thymine and uracil) which will be a subject of future research.

Acknowledgements

The authors would like to thank the BESSY staff members for their assistance during the beam times (especially Mike Sperling for the technical support). We also acknowledge the financial support granted by the BMBF (FK MUSTANG 05KS40C1/3, FK 05KS1OCA1).

References

[1] A.D. Becke, J. Chem. Phys. 98 (1993) 1372.
[2] J.N. Crain, A. Kirakosian, J.-L. Lin, Y. Gu, R.R. Shah, N.L. Abbott, F.J. Himpsel, J. Appl. Phys. 90 (7) (2001) 1.
[3] M.J. Frisch, G.W. Trucks, H.B. Schlegel, G.E. Scuseria, M.A. Robb, J.R. Cheeseman, J.A. Montgomery Jr., T. Vreven, K.N. Kudin, J.C. Burant, J.M. Millam, S.S. Iyengar, J. Tomasi, V. Barone, B. Mennucci, M. Cossi, G. Scalmani, N. Rega, G.A. Petersson, H. Nakatsuji, M. Hada, M. Ehara, K. Toyota, R. Fukuda, J. Hasegawa, M. Ishida, T. Nakajima, Y. Honda, O. Kitao, H. Nakai, M. Klene, X.

Li, J.E. Knox, H.P. Hratchian, J.B. Cross, V. Bakken, C. Adamo, J. Jaramillo, R. Gomperts, R.E. Stratmann, O. Yazyev, A.J. Austin, R. Cammi, C. Pomelli, J.W. Ochterski, P.Y. Ayala, K. Morokuma, G.A. Voth, P. Salvador, J.J. Dannenberg, V.G. Zakrzewski, S. Dapprich, A.D. Daniels, M.C. Strain, O. Farkas, D.K. Malick, A.D. Rabuck, K. Raghavachari, J.B. Foresman, J.V. Ortiz, Q. Cui, A.G. Baboul, S. Clifford, J. Cioslowski, B.B. Stefanov, G. Liu, A. Liashenko, P. Piskorz, I. Komaromi, R.L. Martin, D.J. Fox, T. Keith, M.A. Al-Laham, C.Y. Peng, A. Nanayakkara, M. Challacombe, P.M.W. Gill, B. Johnson, W. Chen, M.W. Wong, C. Gonzalez, J.A. Pople, Gaussian 03, Revision C02, Gaussian, Inc., Wallingford CT, 2004.

[4] S. Gorelsly, AOMix program, revison 5.92, 2004. <http://www.sg-chem.net/>.

[5] S. Gorelsly, A.B.P. Lever, J. Organomet. Chem. 635 (2001) 187.

[6] K. Hinrichs, S.D. Silaghi, C. Cobet, N. Esser, D.R.T. Zahn, Phys. Status Solidi B—Basic Solid State Phys. 242 (13) (2005) 2681.

[7] G. Maruccio, Nano Lett. 3 (2003) 479.

[8] M. Nyberg, Y. Luo, L. Triguero, L.G.M. Pettersson, H. Ågren, Phys. Rev. B 60 (1999) 7956.

[9] H. Oji, R. Mitsumoto, E. Ito, H. Ishii, Y. Ouchi, J. Chem. Phys. 109 (1998) 10409.

[10] M.A. Olmstead, R.D. Bringans, R.I.G. Uhrberg, R.Z. Bachrach, Phys. Rev. B 34 (4) (1986) 6041.

[11] D. Porath, A. Bezryadin, S. de Vries, C. Dekker, Nature 403 (2000) 635.

[12] J. Schnadt, J. Schiessling, P. Brühwiler, Chem. Phys. 312 (2005) 39.

[13] A. Schöll, M. Jung, Th. Schmidt, R. Fink, E. Umbach, J. Chem. Phys. 121 (2004) 10260.

[14] S.D. Silaghi, M. Friedrich, C. Cobet, N. Esser, W. Braun, D.R.T. Zahn, Phys. Status Solidi B—Basic Solid State Phys. 242 (15) (2005) 3047.

[15] P.J. Stephens, F.J. Devlin, C.F. Chabalowski, M.J. Frisch, J. Phys. Chem. 98 (1994) 11623.

[16] J. Stöhr, NEXAFS Spectroscopy, Springer, Berlin, Heidelberg, 1992.

[17] J. Stöhr, D. Outka, Phys. Rev. B 36 (1992) 7891.

[18] R.I.G. Uhrberg, T. Kaurila, Y.-C. Chao, Phys. Rev. B 58 (4) (1998) R1730.

[19] D.R.T. Zahn, S.D. Silaghi, C. Cobet, M. Friedrich, N. Esser, Phys. Status Solidi B—Basic Solid State Phys. 242 (13) (2005) 2671.